A RIF1 and KAP1-based, double-bookmarking system generates a toggle switch that stabilises the identities of the active and inactive X chromosomes during random X inactivation in mouse

Elin Enervald[1,2], Rossana Foti[2,$], Lynn Marie Powell[1], Agnieszka Piszczek[2,£] and Sara C.B. Buonomo[1,2,*]

1 current address: Institute of Cell Biology, School of Biological Sciences University of Edinburgh, Roger Land, Building, Alexander Crum Brown Road, Edinburgh, EH9 3FF, UK.

2 Epigenetics & Neurobiology Unit, European Molecular Biology Laboratory (EMBL Rome), Monterotondo, Italy.

$ current address: Center for Basic and Translational Neuromedicine, Faculty of Health and Medical Sciences, University of Copenhagen, Norrè Alle 14, 24.2.16, 2200 København N, Denmark.

£ current address: HistoPathologyVienna BioCenter Core Facilities (VBCF), Dr. Bohr-Gasse 3, 1030 Vienna, Austria

*Corresponding author and lead contact: sara.buonomo@ed.ac.uk

Keywords: X inactivation, RIF1, KAP1, X chromosome choice, Tsix, Xist.

ABSTRACT

Dosage compensation for the X chromosome-linked genes in female placental mammals is achieved through the random silencing of one of the two X chromosomes. The onset of random X inactivation in mouse embryos and in differentiating embryonic stem cells requires the switch from a symmetric state, where both X chromosomes are equivalent, to an asymmetric state, where the identity of the future inactive and active X chromosomes are assigned. This “choice”, initiated by a stochastic event, needs to evolve into a stable and transmissible state. The transition from bi- to mono-allelic expression of the long non-coding RNA Tsix is thought to be one of the initial events breaking the symmetry of the two X chromosomes. Here we show that the asymmetric expression of *Tsix* triggers in turn the switch of RIF1 association with the *Xist* promoter from dynamic and symmetric to stable and asymmetric (on the future inactive X). On the future inactive X, RIF1 then plays an essential role in the upregulation of *Xist*, thus initiating the consolidation and stable transmission of the identity of the inactive X. Tsix-dependent exclusion of RIF1 from the future active X chromosome in turn permits the association of KAP1 with the *Xist* promoter, thus marking the future active X chromosome. Timely mono-allelic association of KAP1 is important for a stable choice and for X inactivation. We present here a double-bookmarking system, based on the mutually exclusive relationships of Tsix and RIF1, and RIF1 and KAP1. This system coordinates the identification of the active and inactive X chromosomes and initiates a self-sustaining loop that transforms an initially stochastic event into a stably inherited asymmetric X chromosome state.

INTRODUCTION

Random X chromosome inactivation (XCI) is the process leading to the stable transcriptional silencing of one of the two X chromosomes in female placental mammals, with the aim of equalising the expression of X-linked genes between males and females[1]. This process represents one of the best-studied examples of how different nuclear processes, such as epigenetic control, 3D organisation of chromatin contacts, sub-nuclear positioning and, potentially, replication-timing regulation, are integrated to achieve transcriptional control. Random XCI is initiated when Xist, an X-encoded long non-coding RNA (lncRNA) is upregulated from one of the two X chromosomes, the future inactive X chromosome (Xi)[2-5]. *In vivo,* this happens around the time of embryo implantation[6,7], while in cultured female mouse embryonic stem cells (mESCs), XCI takes place during a narrow time-window at the onset of differentiation[8]. Monoallelic upregulation of *Xist* is coupled to loss of pluripotency and several activating and repressing factors of this process have been described[9-16]. Guided by the X chromosome three-dimensional (3D) conformation[17,18], Xist spreads *in cis*, promoting Polycomb-dependent tri-methylation of H3K27 (H3K27me3)[19,20], tethering of the future inactive X chromosome (Xi) to the nuclear periphery[21], exclusion of RNA polymerase II[22,23], and the switch of the replication timing of the entire Xi to mid-late S-phase[24]. An exceptionally stable transcriptionally silent status is thus achieved, so robustly controlled that is maintained throughout the entire life of the organism. One of the least understood of all these steps is the mechanism that in the initiating phase, directs the random choice of which one of the two *Xist* alleles to upregulate, marking the future Xi, and which to silence (marking the future active X chromosome, Xa). We will refer to this process as the “choice”. This is a key stage, as failure to establish monoallelic *Xist* expression can result in either both X

chromosomes being silenced or both remaining active, consequently leading to embryonic lethality[4,25,26]. Tsix is a lncRNA encoded by a gene that overlaps, in the antisense orientation, with *Xist* and plays a well-established role as an *in cis* repressor of *Xist*. In female mESCs, *Tsix* is biallelically expressed, to become downregulated on one of the two X chromosomes, the future Xi, at the onset of differentiation, hence allowing for *in cis Xist* upregulation[27,28]. The switch to mono-allelic expression of *Tsix* is important in assigning the destinies of the future Xi (Tsix silenced) and Xa (Tsix maintained). In fact, interfering with the expression of one of the two *Tsix* alleles in female mESCs results in a non-random choice, with the *Tsix*-defective chromosome predetermined as the future Xi (reviewed in[29]). On the other hand, homozygous deletion of *Tsix* leads to a 'chaotic' XCI, with a mixture of cells showing either no *Xist* upregulation or biallelic upregulation during differentiation[30]. Although *Tsix* downregulation is essential for *in cis* upregulation of Xist, the molecular mechanism of Tsix-driven silencing is still unclear. The *Tsix* terminator region overlaps with the *Xist* promoter, and *Tsix* transcription through this region and/or Tsix RNA have been proposed to be important for *Xist* repression[31] by promoting a silenced chromatin state[32-35]. The establishment of the opposite *Xist/Tsix* expression patterns on the two genetically identical X chromosomes, must rely on the coordinated asymmetric distribution of activators and/or repressors of transcription.

Mathematical modeling can recapitulate the experimental features of XCI by postulating the existence of an *in cis* negative regulator of *Xist* (cXR) and an *in trans*, X-linked, *Xist* activator (tXA)[36]. While a cXR is sufficient to explain the maintenance of mono-allelic *Xist* expression, a tXA is needed to explain 1. the establishment of the *Xist* mono-allelic expression; 2. the female specificity of XCI; 3. the resolution of bi-allelic *Xist* expression detected, to various extents, in different organisms[36]. In mouse,

the cXR is probably Tsix while RNF12, an X-linked ubiquitin ligase that functions as a dose-dependent trigger of XCI[12,14], has been proposed as a tXA. However, while over-expression of RNF12 in male cells can induce XCI[12], its deletion in females is not sufficient to prevent *Xist* upregulation[37,38]. Thus, RNF12 could account for the X-linked aspects of the tXA function, such as female specificity and resolution of bi-allelic expression, but one or multiple other transactivator/s must be contributing to the control of *Xist*. Moreover, conceptually, the expression level of a single, X-linked gene, does not constitute a switch robust or sensitive enough to be the only element to control a clear-cut bi-stable state for *Xist* (active on one and silent on the other allele). The establishment of *in cis*, self-reinforcing and mutually exclusive circuits on the two *Xist* alleles could create the ultrasensitivity required to generate a binary switch-type of control[39]. Key to this model, is the idea that the initial stochastic events will trigger a chain of local, mutually exclusive and self-sustaining events to bookmark both Xi and Xa.

RIF1 is a multifaceted protein, required for the regulation of several of the nuclear processes that take place during XCI. RIF1 is the only known genome-wide regulator of replication timing[40-46], it confines long-range chromatin contacts within the respective boundaries of the nuclear A/B compartments[47] and plays an as yet unclear function in the control of gene expression[45,48-52]. RIF1 is an adaptor for Protein Phosphatase 1 (PP1), one of the main Ser/Thr phosphatases in eukaryotic cells[42,53-58]. In *Drosophila melanogaster,* this interaction was shown to be essential during embryonic development[46]. In addition, the RIF1-PP1 interaction is essential for RIF1-dependent organisation of chromatin contacts[47]. Others[52,59] and we (this work) have observed that mouse RIF1 deficiency is associated with a sex-linked differential

lethality, with the female embryos dying around the time of implantation. These data have suggested that RIF1 could be important during XCI. Here we find that RIF1, present biallelically on the *Xist* P2-promoter in mESCs, becomes asymmetrically enriched at P2 on the future Xi, concomitant with the choice, at the time when *Tsix* expression switches from bi- to mono-allelic. On the future Xi, RIF1 plays then an essential role for *Xist* upregulation. RIF1 removal allows the binding of KAP1 (KRAB-associated protein 1, also known as TRIM28 and TIF1β), whose timely association with the future Xa is also important for the onset of XCI. Our data identify the asymmetric binding of RIF1, and, consequently, of KAP1, as a key step in the molecular cascade that leads to the bookmarking of the future Xi and Xa, thus implementing a stable binary state for Xist.

RESULTS

RIF1 is required for X inactivation during embryonic development and for *Xist* upregulation

The analysis of the progeny derived from inter-crosses of mice heterozygous for a *Rif1* null allele (*Rif1*$^{+/-}$, Fig. S1A and B) in a pure C57BL/6J genetic background has revealed that *Rif1* is essential for embryonic development (Fig. 1A). In contrast, in a mixed genetic C57BL/6J-129/SvJ background, *Rif1* deletion results in a differential lethality between the sexes (Fig. 1B). Indeed, in this case, only a small proportion of the expected *Rif1*$^{-/-}$ mice, exclusively males, are recovered at weaning. In order to pinpoint more precisely the time of the onset of lethality, we have analysed the viability of *Rif1*$^{-/-}$ embryos at different stages of development in a C57BL/6J pure background. We found that, up to the blastocyst stage, there are no obvious differences between

male (data not shown) and female *Rif1* null and wild type embryos (Fig. S2A). However, immediately after implantation (E5.5), the female embryos show a dramatically reduced expansion of the epiblast (Fig. S2B) and are already dead by E7.5 (Fig. 1C and D). In contrast, males appear to die only around mid-gestation (Fig. 1C). This early-onset lethality observed specifically in females suggests that the lack of RIF1 could interfere with the process of XCI, as the timing coincides with the onset of random XCI.

Given the diversity of its roles, RIF1 could act at one or several of the multiple steps during XCI. To dissect at what stage(s) of the process RIF1 is required, we generated female mESCs carrying homozygous conditional *Rif1* allele ($Rif1^{Flox/Flox}$) and a tamoxifen-inducible CRE recombinase ($Rosa26^{Cre\text{-}ERT/+}$,[60]). To trigger XCI in the absence of *Rif1*, we have set up a protocol in which we combined differentiation by embryoid bodies (EB) formation[61] and tamoxifen treatment (Fig. 2A). We found that *Rif1* deletion (Fig. 2B) severely impairs *Xist* upregulation (Fig. 2C and S3A) and, consequently, the enrichment of H3K27me3 on the future Xi (Fig. 2D). Failure of *Xist* upregulation in the absence of *Rif1* is not due to a general defect in exit from pluripotency (Fig. S3B) or to failed commitment to differentiation (Fig. S3C). Moreover, the main negative regulator of Xist, Tsix appears reduced in *Rif1* knockout cells during the early stages of differentiation, when *Xist* normally is upregulated (Fig. S4A). Finally, the overall dynamics of RNF12 appear comparable between control and *Rif1* knock out cells (Fig. S4B), Overall, these results indicate that failure of *Xist* upregulation is the likely cause of defective XCI in *Rif1* null female embryos and that RIF1 could directly and positively regulate *Xist* expression.

RIF1 is a positive regulator of *Xist* and its binding specifically bookmarks the future Xi

Xist is controlled from two promoters, P1 and P2, separated by a repetitive region essential for the silencing properties of Xist[62]. While the upstream P1 promoter gives rise to the Xist main transcript, P2 appears to serve as an internal regulatory unit, possibly controlling P1 expression[15]. We found that RIF1 is enriched specifically at *Xist* P2 promoter, both in mESCs (Fig. 3A) and in early EBs (Fig. 3B), supporting the hypothesis that RIF1 could be a direct regulator of *Xist* expression. Upon differentiation, *Xist* is transcribed mono-allelically, upregulated only from the future Xi. If RIF1 is a positive regulator of *Xist*, we would expect it to be associated mono-allelically, specifically with P2 on the future Xi. In order to test this hypothesis, we have taken advantage of the Fa2L cell line, in which 1. the two X chromosomes can be discriminated, as one originates from *Mus castaneus* (*cast*) and the other from *Mus musculus 129/SvJ* (*129*) mouse strains; 2. Xa (*cast*) and Xi (*129*) are predetermined already in ESCs, as the *129 Tsix* allele carries a transcriptional stop signal, approximately 4kb downstream from the *Tsix* major promoter[63]. *Xist* is therefore preferentially upregulated from the *129*-derived X chromosome. We have analysed the association of RIF1 with *Xist* P2 promoter of the future Xa and Xi by allele-specific ChIP-qPCR (Fig. S5A) and found that RIF1 is preferentially associated with the *Xist* P2 promoter of the*129 Xist* allele (future Xi, Fig. 3C). Importantly, in control wild type mESCs (bi-allelically expressed *Tsix*), also carrying one *cast* and one *129* X chromosome, RIF1 is equally distributed on both P2 promoters (Fig. 3C), suggesting that the asymmetric association with the future Xi is concomitant with the switch from bi- to mono-allelic *Tsix* expression that accompanies the choice and allows *Xist* monoallelic upregulation. As in the case of RIF1 conditional cells, depletion of RIF1 in

Fa2L cells (Fig. S5B) also compromises *Xist* upregulation (Fig. S5C). These data show that RIF1 asymmetric association with the future Xi parallels the choice and it is essential for *Xist* upregulation.

KAP1 association with the future Xa is important for the onset of XCI

With the aim of understanding the molecular mechanism by which RIF1 regulates *Xist* expression, we have investigated whether some of the known transcriptional regulators associated with RIF1 are also required for XCI. We focused in particular on KAP1, as KAP1 and RIF1 have already been shown to regulate overlapping targets, such as Dux and MERVLs[48,64,65]. We found that knock down of KAP1 (Fig. 4A and B) impairs *Xist* upregulation (Fig. 4C), similarly to the knockout of *Rif1*. This is not due to compromised exit from pluripotency (Fig. S6A) or impaired activation of the differentiation transcriptional program (Fig. S6B), suggesting that diminished *Xist* activation is not a consequence of an overall impaired cell differentiation. In addition, the dynamics of expression of RNF12 appear comparable between control and KAP1 knock down cells (Fig. S6C). As in *Rif1*$^{-/-}$ cells, in KAP1 knock down cells Tsix levels do not undergo a transient increase during the initial stages of differentiation that we have seen in the control cells (Fig. S6D). These data suggest that KAP1 could indeed collaborate with RIF1 to allow *Xist* expression from the future Xi. In order to further investigate this hypothesis, we analysed KAP1 distribution on the future Xa and Xi in the Fa2L cells. Surprisingly, we found that RIF1 and KAP1 show a complementary pattern of association with *Xist* promoter. While RIF1 is preferentially associated with the *129 Xist* allele (future Xi, Fig. 3C), KAP1, instead, displays preferential association with the *castaneus Xist* allele (future Xa, Fig. 4D) Moreover, in the control mESCs, where *Tsix* is bi-allelically expressed, KAP1 is barely detectable on *Xist* P2 above the

levels seen for the intergenic regions (Fig. 4D). These data indicate that, unlike RIF1, which associates with *Xist* P2 prior to the choice, to then become specifically enriched on the Xi when *Tsix* is mono-allelically expressed, KAP1 association with *Xist* promoter (on the future Xa) takes place only when *Tsix* is mono-allelically expressed. KAP1 could be important *in cis*, to promote or consolidate the transition from bi- to mono-allelic expression of *Tsix*, thus marking the future Xa. Failure to achieve monoallelic *Tsix* expression results in an aberrant *Xist* upregulation where only a fraction of the cells will upregulate *Xist* correctly[30], potentially explaining our observation that knock down of KAP1 (Xa-associated) results in compromised *Xist* upregulation from the Xi. In order to investigate whether KAP1 is important at the time of transition from bi- to mono-allelic *Tsix* expression, we employed the Fa2L cells. In these cells, *Tsix* truncation artificially creates *Tsix* mono-allelic expression already in mESCs, effectively creating a post-choice situation. If KAP1 is required to promote a stable switch from bi- to mono-allelic *Tsix* expression, we would expect that KAP1 knock down in Fa2L cells would have no consequences on *Xist* upregulation. Confirming our hypothesis, we found that KAP1 knock down (Fig. S7A) does not affect *Xist* (Fig. 4E and S7B) or *Tsix* expression (Fig. S7C) in the Fa2L cells.

RIF1 negatively regulates KAP1 association with Xist promoter in mESCs

Our data show that when *Tsix* becomes mono-allelically expressed, during the choice, RIF1 asymmetric association to the future Xi parallels the asymmetric binding of KAP1 on the future Xa, suggesting the existence of a double-bookmarking system to identify the future Xi/Xa. In order to understand if and how these two systems are coordinated, we have investigated whether RIF1 regulates KAP1 association with *Xist* P2. KAP1 is barely detectable on the *Xist* promoter in wild type mESCs and gains association early

upon differentiation (Fig. 5A), in agreement with its proposed role during the choice. Moreover, we found that *Rif1* deletion leads to earlier KAP1 binding to *Xist* promoter, as it becomes already evident in mESCs (Fig. 5B). This is not due to a general increase of the steady-state levels of KAP1 (Fig. S8A) or its overall binding to chromatin (Fig. S8B). Moreover, KAP1 enrichment is specific for *Xist* promoter, as neither of the other regions known to be associated with KAP1 that we have tested, Znf629 and Ezr[66], show an increased KAP1 association upon *Rif1* deletion. Importantly, the effect of RIF1 deficiency is not due to an indirect, general remodelling of the *Xist* promoter, as the association of another P2-specific transcription factor and *Xist* activator, Yin-Yang-1 (YY1)[15], is unchanged in *Rif1* knockout cells (Fig S8C). We also found that knocking down RIF1 in the Fa2L cells (Fig. 5C) affects KAP1 association to *Xist* P2 (Fig. 5D) comparably to what happens in *Rif1* conditional cells upon induction of *Rif1* deletion (Fig. 5B). In this case, we could also determine that KAP1 gains access specifically to the future Xi (*129* allele, carrying the truncated *Tsix* allele), where normally RIF1 is preferentially localised (Fig. 3C). Overall, these data indicate that, in mESCs, RIF1 is symmetrically associated with *Xist* P2 on both X chromosomes, protecting P2 from the binding of KAP1. When *Tsix* is mono-allelically expressed, RIF1 is asymmetrically associated with *Xist* promoter on the future Xi, where it plays an essential role for *Xist* upregulation. The asymmetric distribution of RIF1, in turn allows the association of KAP1 with *Xist* promoter on the future Xa. KAP1 association with *Xist* P2 on the future Xa is important prior to or concomitantly with *Tsix* switching to a mono-allelic expression, as KAP1 is dispensable in cells in which *Tsix* is artificially expressed mono-allelically.

RIF1 asymmetric localisation on the future Xi is driven by *Tsix* expression

How is the transition from bi- to mono-allelic RIF1 association with *Xist* promoter regulated? While usually this is triggered by differentiation, in undifferentiated Fa2L cells it has already taken place and RIF1 is preferentially associated with the X chromosome that does not express full-length Tsix transcript (Fig. 3C). This suggests that Tsix RNA and/or transcription could destabilise RIF1 association with *Xist* promoter. In agreement with this hypothesis, we found that blocking *Tsix* expression by treating the Fa2L cells with the CDK9-inhibitor flavopiridol[67] (Fig. S8D), is sufficient to revert RIF1 preferential association with the future Xi to a symmetric mode of binding (Fig. 5E). In addition, flavopiridol treatment of wild type ESC also leads to an increased P2-association of RIF1 (Fig. 5F), suggesting that bi-allelic ongoing transcription or Tsix RNA itself contribute to a dynamic RIF1 association to P2 in mESCs.

DISCUSSION

While marsupials have adopted an imprinted X inactivation strategy, eutherians have evolved a mechanism based on the random choice of the X chromosome to be inactivated. The latter can contribute to a higher degree of resistance of females to pathogenic X-linked mutations and increase phenotypic diversity. Despite its importance, the mechanisms guiding the random choice are still unclear, partially because of the randomness and consequent heterogeneity in the cell population, partially because of the inaccessibility of the early embryos, where the process takes place naturally and, finally, because of the inherent difficulty of identifying asymmetry involving two identical chromosomes.

Several lines of evidence suggest that *Tsix* is involved in the choice-making process. For example, introduction of a stop that blocks Tsix transcript before its overlap with *Xist*[63], or deletions of its major promoter[68] or the GC-rich repeat region that immediately follows it (Dxpase34)[9], result in a non-random choice, with the *Tsix*-defective chromosome as the future Xi. Moreover, monoallelic downregulation of Tsix levels by deleting *Xite*, a *cis*-acting element that positively regulates *Tsix*, also skews the choice[69]. Interestingly, Xist itself can influence the choice, in a yet-to-be-understood feedback control loop. *Xist* ectopic upregulation can in fact skew the choice in favour of the *Xist*-overexpressing chromosome[70,71].

Our experiments show that RIF1 association with the *Xist* P2 promoter is negatively regulated by *Tsix* expression. *Tsix* expression could therefore be the determinant of the asymmetric association of RIF1 with the future Xi following/at-the-choice. When cells commit to differentiation, the dynamic association of RIF1 could become frozen in an asymmetric state, reflecting the ongoing transcriptional state of *Tsix* at the moment of commitment. We would like to propose a model (Fig. S9) whereby at the onset of differentiation, asymmetric levels of Tsix would lead to breaking the symmetry of RIF1 association with *Xist* P2. The asymmetry of Tsix levels could be initiated by the stochastic expression of *Tsix* from one of the two alleles or by the stochastic upregulation of *Xist* from one allele, that would, in turn, lead to a *in cis* decrease in Tsix levels. This transient asymmetry would leave RIF1 marking the future Xi and would permit a more stable KAP1 association with the future Xa. This would initiate a self-reinforcing loop on the future Xa, with KAP1 promoting preferential *in cis* transcription of *Tsix*. In support of this model, we have identified a transient increase in Tsix levels in the initial stages of differentiation, preceding *Xist* upregulation, that is

suppressed by the pre-choice knock down of KAP1 (Fig. S6D) or, in the absence of RIF1 (Fig. S4A), when KAP1 precociously associates with *Xist* P2 in mESCs (Fig. 5B). One of the limitations of any model based on mouse *Tsix* function is its applicability to other model systems, where *Tsix* role has not been clearly shown, although it has not been excluded either. For example, in human cells, the lncRNA XACT has been proposed as a potential Tsix-like negative regulator of *Xist*[72,73]. One unique feature of the mouse *Tsix/Xist* gene pair is the extended overlap of the two genes, which is a requirement if RIF1 depletion from the future Xa is due to *Tsix* transcription. However, RIF1 was recently isolated in a large screen for RNA associated proteins[74] raising the possibility that Tsix RNA or any functional equivalent in other species, could work as an RNA platform to titrate away RIF1.

The negative effect of RIF1 on KAP1 association with *Xist* promoter is at the heart of the mutual exclusion, reinforced by KAP1's positive effect on the levels of Tsix, that is, in turn, a negative regulator of RIF1 association with *Xist* promoter. How RIF1 excludes KAP1 is currently unclear, but we can envisage at least two potential mechanisms, based either on RIF1/KAP1 competition for binding to a shared site or protein partner, or through KAP1 de-phosphorylation by RIF1-associated PP1. Phosphorylation of KAP1 has indeed been shown to regulate KAP1 association with heterochromatin protein 1 (HP1)[75].

Our data suggest that KAP1's association with the *Xist* promoter on the future Xa is important to sustain *Tsix* expression *in cis*, at least in the initial stages of the establishment of the asymmetry of the two X chromosomes. Although better known as a transcriptional repressor, KAP1 has also been implicated in the positive control of transcription, by promoting the release of RNA polymerase II from transcriptional

start site (TSS)-proximal pausing[76]. This function of KAP1 is exerted as part of the 7SK complex[77], a ribonucleoprotein complex with roles at both the promoter and transcriptional termination of several genes, including several lncRNAs[78]. The region of KAP1 association with the *Xist* promoter coincides with the *Tsix* terminator in the opposite orientation. It is therefore possible that KAP1, as a part of the 7SK complex, could promote the establishment of a terminator-promoter positive feedback loop[79], that would maintain *in cis* the expression of *Tsix* during the initial stages of differentiation. In support of this hypothesis, we have found that the 7SK complex is also enriched on *Xist* promoter/*Tsix* terminator in *Rif1* knockout mESCs, in a KAP1-dependent manner (unpublished data).

The overlap between *Tsix* terminator and *Xist* promoter raises the possibility that KAP1 could also, in addition to promoting *Tsix* expression, repress *Xist* promoter on the same chromosome. KAP1's best known repressive function is mediated through its interaction with SetDB1, an HMTase that tri-methylates K9 on histone H3. We did not find the gain of H3K9me3 observed in wild type Fa2L cells on the *Xist* promoter of the Xa, to be affected by KAP1 knock down. However, this result could have multiple explanations, from the intervals between the timepoints that we have analysed, to the specific use of the Fa2L cells. As these cells represent an artificial post-choice system, where KAP1 function is dispensable for X inactivation, we could be missing key events taking place at the time of the choice.

Another surprising finding of this work is the identification of RIF1 as a positive regulator of *Xist* expression. Although we have previously shown that RIF1 is associated with a number of GC-rich TSSs in mESCs[45], most of the evidence linking RIF1 to gene expression suggests its function as a negative regulator[48-52]. In general,

RIF1 is associated with silenced chromatin regions, raising the question of what the molecular mechanism of this positive control could be. One hypothesis is that RIF1 primarily shields *Xist* promoter from the repressive effects of KAP1 association. However, this would not explain why KAP1 depletion in the Fa2L cells does not lead to bi-allelic *Xist* upregulation (Fig. S7B). Importantly, KAP1 depletion in these cells is not sufficient for RIF1 to regain access to Xist P2 on the *cast* allele, normally bound by KAP1 (unpublished data). This observation supports the hypothesis that RIF1 plays a role as an essential, positive regulator of *Xist*, in addition to its role in controlling KAP1 association with *Xist* P2.

In summary, we propose that, during the stochastic phase of the choice of the future Xi, the asymmetric distribution of RIF1, following a Tsix-dependent stripping from the future Xa, triggers the establishment of two, mutually exclusive, *in cis* circuits that will identify Xi and Xa. RIF1's presence on P2, inhibiting KAP1 and promoting *Xist* expression on Xi, and KAP1's presence on P2, sustaining Tsix levels and, thus, helping to exclude RIF1 from Xa, would evolve the initial stochastic event of Tsix asymmetry into a binary switch, where a bi-stable, self-sustaining situation on the two X chromosomes is propagated.

Acknowledgments

We would like to acknowledge David Kelly from the COIL facility, WTCCB, University of Edinburgh; Emerald Perlas from the Histology Facility of the Epigenetics & Neurobiology Unit, EMBL Rome; Violetta Parimbeni for mouse husbandry, (Epigenetics & Neurobiology Unit, EMBL Rome). We would like to thank Phil Avner

and Andrea Cerase (Epigenetics & Neurobiology Unit, EMBL Rome) for advice, reagents, support, discussions and critically reading the manuscript. Rafael Galupa (EMBL Heidelberg) and Jacqueline Mermoud (University of Marburg) are thanked for critically reading the manuscript. Titia de Lange (The Rockefeller University) is thanked for initially supporting the generation of the *Rif1* knockout mice. EE received funding from the European Union's Horizon 2020 research and the Marie Skłodowska-Curie Individual Fellowship grant agreement No. 660985 and from the ERC consolidator award 726130 to SCBB. RF was funded by the EMBL Interdisciplinary Postdoc (EIPOD) fellowship under Marie Curie Actions (COFUND). LP is funded from the ERC consolidator award 726130 to SCBB.

Author Contributions

EE has created the cellular system, performed the majority of the experiments and co-written the manuscript. RF initiated the project and performed some of the early experiments, like the staining of E3.5 embryos. LP has supported some of the experiments. AP has isolated and stained the E5.5 embryos. SCBB has conceived the project, performed some of the experiments and written the manuscript.

Declaration of Interests

The authors declare no competing interests.

FIGURE LEGENDS

Figure 1. *Rif1* deficiency leads to female embryonic lethality at peri-implantation. Tables summarising the number and the sexes of the pups recovered at weaning from *Rif1*$^{+/-}$ x *Rif1*$^{+/-}$ mice inter-crosses, either in a C57BL/6J **(A)** or in a mixed C57BL/6J-129/SvJ genetic background **(B)**. The observed number of mice is compared to the

expected number, based on the Mendelian ratio. *p* calculated by Student's *t* test. **(C).** The table summarises the number and the sex of the embryos of the indicated genotypes, recovered from timed matings of *Rif1*$^{+/-}$ x *Rif1*$^{+/-}$ mice, in a C57BL/6J genetic background. The day of gestation (E) is indicated (**D)** Representative images of *Rif1*$^{-/-}$ E7.5 embryos, female top and male bottom.

Figure 2. *Rif1* null female mESCs fail to upregulate *Xist* upon differentiation.

(A). Overview of the experimental design. *Rif1*$^{+/+}$ and *Rif1*$^{F/F}$ mESCs were grown for two days in medium supplemented with 4-Hydroxytamoxifen (OHT) to induce the translocation into the nucleus of the Cre-recombinase, leading to *Rif1* deletion in the Rif1$^{F/F}$ cells (*Rif1*$^{-/-}$). The embryoid body (EB) differentiation protocol was then started to trigger XCI. OHT was kept in the medium during the first 24 hours of EB differentiation. Cells were differentiated up to 4 (RNA analysis) or 7 days (H3K27 IF). **(B).** Representative western blot to monitor RIF1 levels after Cre-mediated *Rif1* deletion and EB differentiation. SMC1: loading control. **(C).** Time course analysis of Xist RNA expression by RT-qPCR during EB differentiation of *Rif1*$^{+/+}$ and *Rif1*$^{-/-}$ cells at the indicated timepoints. *Rif1*$^{+/+}$ (solid line) and *Rif1*$^{-/-}$ (dashed line), female (black) and male (grey). Data are presented as mean ± standard deviation (SD) from three (female lines) two (male lines) independent experiments. Xist RT-primers Xist ex7 F and R were used. Values are normalised to a geometric mean consisting of the expression of *Gapdh*, *Ubiquitin* and *β-Actin*. **(D).** Bar plot summarising the number of cells showing H3K27me3-marked Xi as a percentage of total cells counted, in *Rif1*$^{+/+}$ and *Rif1*$^{-/-}$ mESCs at the indicated days of EB differentiation. Averages ±SD from three (day 4 and 7) and two (day 2) independent experiments (n>200).

Figure 3. RIF1 associates with *Xist* promoter on the future Xi.

RIF1 association with the *Xist* promoter assessed by ChIP-qPCR in two independent *Rif1*$^{+/+}$ (black) and two *Rif1*$^{-/-}$ (grey) cell lines, in mESCs **(A)** and at 2 days of EB differentiation **(B)**. P1 and P2 indicate the two *Xist* promoters, 5' indicates a region 2 kb upstream of *Xist* TSS. Inter1 and 2 are two intergenic regions that serve as negative controls. Peak and cRAD represent two previously identified regions of RIF1 association (positive control). **(C)** Association of RIF1 with *Xist* P2 in the Fa2L cells (black) and a wild type mESC line, also harbouring one *castaneus* and one *129* X chromosome (grey). Allele-specific ChIP-qPCR primers were used *cast* indicates association with the *castaneus Xist* P2 and *129* indicates association with the *129 Xist* P2. Enrichments are presented relative to input DNA. Mean ±SD from 3 independent experiments (A and C) and 2 independent experiments (B). *p* calculated by Student's *t* test.

Figure 4. KAP1 associates with *Xist* promoter on the future Xa.

(A). Schematic of the experimental design. **(B).** Western blot analysis of KAP1 levels after knock down, in mESCs and during EB differentiation. SMC1: loading control. (**C**). Time course analysis of *Xist* expression by RT-qPCR during EB differentiation of cells following knock down of Luciferase (Control) (black) and KAP1 (grey), at the indicated timepoints. Data are presented as mean ±SD from three independent experiments. *Xist* primers Xist ex3 F and Xist ex4 R were used. Normalisation was performed using a geometric mean consisting of the expression of *Rplp0, Ubiquitin* and *Sdha*. **(D).** Using allele-specific primers, ChIP-qPCR was used to measure the association of KAP1 with *Xist* P2 in the Fa2L cells (black) and a wild type mESC line (WT-grey) also harbouring one *castaneus* and one *129* X chromosome. *cast* indicates association

with the *castaneus Xist* P2 and *129* indicates association with the *129 Xist* P2. Enrichments are presented relative to input DNA. Mean ±SD from a minimum of three independent experiments. *p* was calculated by Student's *t* test. **(E)**. RT-qPCR analysis of *Xist* expression levels following KAP1 knock down, like (C), but for the Fa2L cell line.

Figure 5. *Tsix* expression controls Rif1 association with Xist P2.

(A). ChIP-qPCR analysis of KAP1 association to the indicated sites in wild type female mESCs and during early differentiation. ZFP629 is a well-characterised KAP1 associated region (positive control). **(B)**. KAP1 association with *Xist* promoter in two independent *Rif1*$^{+/+}$ (black) and two *Rif1*$^{-/-}$ (grey) mESC cell lines. Ezr is an additional region known to associated with KAP1 in mESCs. Enrichments are presented relative to input DNA. Mean ±SD from a minimum of three independent experiments are displayed. *p* calculated by Student's *t* test. **(C).** Western blot analysis of RIF1 levels in protein extracts from Fa2L cells after RIF1 knock down. SMC1: loading control. (**D**)**.** Allele-specific KAP1 association with *Xist* P2 in Fa2L cells following knock down of Luciferase (Control-black) and RIF1 (grey). *cast* indicates association with the *castaneus Xist* P2 promoter and *129* indicates association with the *129 Xist* P2 promoter. Enrichments are presented relative to input DNA. Average ±SD of two independent experiments **(E)**. Quantification by ChIP-qPCR of RIF1 association with the indicated regions in the Fa2L cell line, following treatment with DMSO only (black) or flavopiridol (grey). Primers as in (D). **(F)** Same as in (E) but for a wild type mESC line. All enrichments are presented relative to input DNA. Mean ±SD from three (E) and two (F) independent experiments are presented. *p* calculated by Student's *t* test in (E).

REFERENCES

1 Lyon, M. F. Gene action in the X-chromosome of the mouse (Mus musculus L.). *Nature* **190**, 372-373, doi:10.1038/190372a0 (1961).

2 Brockdorff, N. *et al.* Conservation of position and exclusive expression of mouse Xist from the inactive X chromosome. *Nature* **351**, 329-331, doi:10.1038/351329a0 (1991).

3 Brown, C. J. *et al.* A gene from the region of the human X inactivation centre is expressed exclusively from the inactive X chromosome. *Nature* **349**, 38-44, doi:10.1038/349038a0 (1991).

4 Marahrens, Y., Panning, B., Dausman, J., Strauss, W. & Jaenisch, R. Xist-deficient mice are defective in dosage compensation but not spermatogenesis. *Genes Dev* **11**, 156-166, doi:10.1101/gad.11.2.156 (1997).

5 Penny, G. D., Kay, G. F., Sheardown, S. A., Rastan, S. & Brockdorff, N. Requirement for Xist in X chromosome inactivation. *Nature* **379**, 131-137, doi:10.1038/379131a0 (1996).

6 Monk, M. & Harper, M. X-chromosome activity in preimplantation mouse embryos from XX and XO mothers. *J Embryol Exp Morphol* **46**, 53-64 (1978).

7 Rastan, S. Timing of X-chromosome inactivation in postimplantation mouse embryos. *J Embryol Exp Morphol* **71**, 11-24 (1982).

8 Wutz, A. & Jaenisch, R. A shift from reversible to irreversible X inactivation is triggered during ES cell differentiation. *Mol Cell* **5**, 695-705, doi:10.1016/s1097-2765(00)80248-8 (2000).

9 Lee, J. T. & Lu, N. Targeted mutagenesis of Tsix leads to nonrandom X inactivation. *Cell* **99**, 47-57, doi:10.1016/s0092-8674(00)80061-6 (1999).

10 Tian, D., Sun, S. & Lee, J. T. The long noncoding RNA, Jpx, is a molecular switch for X chromosome inactivation. *Cell* **143**, 390-403, doi:10.1016/j.cell.2010.09.049 (2010).

11 Furlan, G. *et al.* The Ftx Noncoding Locus Controls X Chromosome Inactivation Independently of Its RNA Products. *Mol Cell* **70**, 462-472 e468, doi:10.1016/j.molcel.2018.03.024 (2018).

12 Jonkers, I. *et al.* RNF12 is an X-Encoded dose-dependent activator of X chromosome inactivation. *Cell* **139**, 999-1011, doi:10.1016/j.cell.2009.10.034 (2009).

13 Navarro, P. *et al.* Molecular coupling of Xist regulation and pluripotency. *Science* **321**, 1693-1695, doi:10.1126/science.1160952 (2008).

14 Gontan, C. *et al.* RNF12 initiates X-chromosome inactivation by targeting REX1 for degradation. *Nature* **485**, 386-390, doi:10.1038/nature11070 (2012).

15 Makhlouf, M. *et al.* A prominent and conserved role for YY1 in Xist transcriptional activation. *Nat Commun* **5**, 4878, doi:10.1038/ncomms5878 (2014).

16 Chureau, C. *et al.* Ftx is a non-coding RNA which affects Xist expression and chromatin structure within the X-inactivation center region. *Hum Mol Genet* **20**, 705-718, doi:10.1093/hmg/ddq516 (2011).

17 Simon, M. D. *et al.* High-resolution Xist binding maps reveal two-step spreading during X-chromosome inactivation. *Nature* **504**, 465-469, doi:10.1038/nature12719 (2013).

18 Engreitz, J. M. *et al.* The Xist lncRNA exploits three-dimensional genome architecture to spread across the X chromosome. *Science* **341**, 1237973, doi:10.1126/science.1237973 (2013).

19 Sun, B. K., Deaton, A. M. & Lee, J. T. A transient heterochromatic state in Xist preempts X inactivation choice without RNA stabilization. *Mol Cell* **21**, 617-628, doi:10.1016/j.molcel.2006.01.028 (2006).

20 Zhao, J., Sun, B. K., Erwin, J. A., Song, J. J. & Lee, J. T. Polycomb proteins targeted by a short repeat RNA to the mouse X chromosome. *Science* **322**, 750-756, doi:10.1126/science.1163045 (2008).

21 Chen, C. K. *et al.* Xist recruits the X chromosome to the nuclear lamina to enable chromosome-wide silencing. *Science* **354**, 468-472, doi:10.1126/science.aae0047 (2016).

22 Chaumeil, J., Le Baccon, P., Wutz, A. & Heard, E. A novel role for Xist RNA in the formation of a repressive nuclear compartment into which genes are recruited when silenced. *Genes Dev* **20**, 2223-2237, doi:10.1101/gad.380906 (2006).

23 Kucera, K. S. *et al.* Allele-specific distribution of RNA polymerase II on female X chromosomes. *Hum Mol Genet* **20**, 3964-3973, doi:10.1093/hmg/ddr315 (2011).

24 Takagi, N., Sugawara, O. & Sasaki, M. Regional and temporal changes in the pattern of X-chromosome replication during the early post-implantation development of the female mouse. *Chromosoma* **85**, 275-286, doi:10.1007/bf00294971 (1982).

25 Borensztein, M. *et al.* Xist-dependent imprinted X inactivation and the early developmental consequences of its failure. *Nat Struct Mol Biol* **24**, 226-233, doi:10.1038/nsmb.3365 (2017).

26 Takagi, N. & Abe, K. Detrimental effects of two active X chromosomes on early mouse development. *Development* **109**, 189-201 (1990).

27 Lee, J. T., Davidow, L. S. & Warshawsky, D. Tsix, a gene antisense to Xist at the X-inactivation centre. *Nat Genet* **21**, 400-404, doi:10.1038/7734 (1999).

28 Stavropoulos, N., Lu, N. & Lee, J. T. A functional role for Tsix transcription in blocking Xist RNA accumulation but not in X-chromosome choice. *Proc Natl Acad Sci U S A* **98**, 10232-10237, doi:10.1073/pnas.171243598 (2001).

29 Starmer, J. & Magnuson, T. A new model for random X chromosome inactivation. *Development* **136**, 1-10, doi:10.1242/dev.025908 (2009).

30 Lee, J. T. Regulation of X-chromosome counting by Tsix and Xite sequences. *Science* **309**, 768-771, doi:10.1126/science.1113673 (2005).

31 Shibata, S. & Lee, J. T. Tsix transcription- versus RNA-based mechanisms in Xist repression and epigenetic choice. *Curr Biol* **14**, 1747-1754, doi:10.1016/j.cub.2004.09.053 (2004).

32 Sado, T., Hoki, Y. & Sasaki, H. Tsix silences Xist through modification of chromatin structure. *Dev Cell* **9**, 159-165, doi:10.1016/j.devcel.2005.05.015 (2005).

33 Navarro, P., Page, D. R., Avner, P. & Rougeulle, C. Tsix-mediated epigenetic switch of a CTCF-flanked region of the Xist promoter determines the Xist transcription program. *Genes Dev* **20**, 2787-2792, doi:10.1101/gad.389006 (2006).

34 Navarro, P., Pichard, S., Ciaudo, C., Avner, P. & Rougeulle, C. Tsix transcription across the Xist gene alters chromatin conformation without affecting Xist transcription: implications for X-chromosome inactivation. *Genes Dev* **19**, 1474-1484, doi:10.1101/gad.341105 (2005).

35 Ohhata, T., Hoki, Y., Sasaki, H. & Sado, T. Crucial role of antisense transcription across the Xist promoter in Tsix-mediated Xist chromatin modification. *Development* **135**, 227-235, doi:10.1242/dev.008490 (2008).

36 Mutzel, V. *et al.* A symmetric toggle switch explains the onset of random X inactivation in different mammals. *Nat Struct Mol Biol* **26**, 350-360, doi:10.1038/s41594-019-0214-1 (2019).

37 Wang, F. *et al.* Rlim-Dependent and -Independent Pathways for X Chromosome Inactivation in Female ESCs. *Cell Rep* **21**, 3691-3699, doi:10.1016/j.celrep.2017.12.004 (2017).

38 Shin, J. *et al.* RLIM is dispensable for X-chromosome inactivation in the mouse embryonic epiblast. *Nature* **511**, 86-89, doi:10.1038/nature13286 (2014).

39 Mutzel, V. & Schulz, E. G. Dosage Sensing, Threshold Responses, and Epigenetic Memory: A Systems Biology Perspective on Random X-Chromosome Inactivation. *Bioessays* **42**, e1900163, doi:10.1002/bies.201900163 (2020).

40 Cornacchia, D. *et al.* Mouse Rif1 is a key regulator of the replication-timing programme in mammalian cells. *EMBO J* **31**, 3678-3690, doi:10.1038/emboj.2012.214 (2012).

41 Hayano, M. *et al.* Rif1 is a global regulator of timing of replication origin firing in fission yeast. *Genes Dev* **26**, 137-150, doi:10.1101/gad.178491.111 (2012).

42 Hiraga, S. *et al.* Rif1 controls DNA replication by directing Protein Phosphatase 1 to reverse Cdc7-mediated phosphorylation of the MCM complex. *Genes Dev* **28**, 372-383, doi:10.1101/gad.231258.113 (2014).

43 Peace, J. M., Ter-Zakarian, A. & Aparicio, O. M. Rif1 regulates initiation timing of late replication origins throughout the S. cerevisiae genome. *PLoS One* **9**, e98501, doi:10.1371/journal.pone.0098501 (2014).

44 Yamazaki, S. *et al.* Rif1 regulates the replication timing domains on the human genome. *EMBO J* **31**, 3667-3677, doi:10.1038/emboj.2012.180 (2012).

45 Foti, R. *et al.* Nuclear Architecture Organized by Rif1 Underpins the Replication-Timing Program. *Mol Cell* **61**, 260-273, doi:10.1016/j.molcel.2015.12.001 (2016).

46 Seller, C. A. & O'Farrell, P. H. Rif1 prolongs the embryonic S phase at the Drosophila mid-blastula transition. *PLoS Biol* **16**, e2005687, doi:10.1371/journal.pbio.2005687 (2018).

47 Gnan, S. *et al.* Nuclear organisation and replication timing are coupled through RIF1-PP1 interaction. *bioRxiv*, 812156, doi:10.1101/812156 (2019).

48 Li, P. *et al.* Rif1 promotes a repressive chromatin state to safeguard against endogenous retrovirus activation. *Nucleic Acids Res* **45**, 12723-12738, doi:10.1093/nar/gkx884 (2017).

49 Tanaka, H. *et al.* Epigenetic Regulation of the Blimp-1 Gene (Prdm1) in B Cells Involves Bach2 and Histone Deacetylase 3. *J Biol Chem* **291**, 6316-6330, doi:10.1074/jbc.M116.713842 (2016).

50 Toteva, T. *et al.* Establishment of expression-state boundaries by Rif1 and Taz1 in fission yeast. *Proc Natl Acad Sci U S A* **114**, 1093-1098, doi:10.1073/pnas.1614837114 (2017).

51 Zofall, M., Smith, D. R., Mizuguchi, T., Dhakshnamoorthy, J. & Grewal, S. I. S. Taz1-Shelterin Promotes Facultative Heterochromatin Assembly at Chromosome-Internal Sites Containing Late Replication Origins. *Mol Cell* **62**, 862-874, doi:10.1016/j.molcel.2016.04.034 (2016).

52 Daxinger, L. *et al.* An ENU mutagenesis screen identifies novel and known genes involved in epigenetic processes in the mouse. *Genome Biol* **14**, R96, doi:10.1186/gb-2013-14-9-r96 (2013).

53 Hiraga, S. I. *et al.* Human RIF1 and protein phosphatase 1 stimulate DNA replication origin licensing but suppress origin activation. *EMBO Rep* **18**, 403-419, doi:10.15252/embr.201641983 (2017).

54 Dave, A., Cooley, C., Garg, M. & Bianchi, A. Protein phosphatase 1 recruitment by Rif1 regulates DNA replication origin firing by counteracting DDK activity. *Cell Rep* **7**, 53-61, doi:10.1016/j.celrep.2014.02.019 (2014).

55 Alver, R. C., Chadha, G. S., Gillespie, P. J. & Blow, J. J. Reversal of DDK-Mediated MCM Phosphorylation by Rif1-PP1 Regulates Replication Initiation and Replisome Stability Independently of ATR/Chk1. *Cell Rep* **18**, 2508-2520, doi:10.1016/j.celrep.2017.02.042 (2017).

56 Mattarocci, S. *et al.* Rif1 controls DNA replication timing in yeast through the PP1 phosphatase Glc7. *Cell Rep* **7**, 62-69, doi:10.1016/j.celrep.2014.03.010 (2014).

57 Sreesankar, E., Bharathi, V., Mishra, R. K. & Mishra, K. Drosophila Rif1 is an essential gene and controls late developmental events by direct interaction with PP1-87B. *Sci Rep* **5**, 10679, doi:10.1038/srep10679 (2015).

58 Trinkle-Mulcahy, L. *et al.* Repo-Man recruits PP1 gamma to chromatin and is essential for cell viability. *J Cell Biol* **172**, 679-692, doi:10.1083/jcb.200508154 (2006).

59 Chapman, J. R. *et al.* RIF1 is essential for 53BP1-dependent nonhomologous end joining and suppression of DNA double-strand break resection. *Mol Cell* **49**, 858-871, doi:10.1016/j.molcel.2013.01.002 (2013).

60 Buonomo, S. B., Wu, Y., Ferguson, D. & de Lange, T. Mammalian Rif1 contributes to replication stress survival and homology-directed repair. *J Cell Biol* **187**, 385-398, doi:10.1083/jcb.200902039 (2009).

61 Doetschman, T. C., Eistetter, H., Katz, M., Schmidt, W. & Kemler, R. The in vitro development of blastocyst-derived embryonic stem cell lines: formation of visceral yolk sac, blood islands and myocardium. *J Embryol Exp Morphol* **87**, 27-45 (1985).

62 Wutz, A., Rasmussen, T. P. & Jaenisch, R. Chromosomal silencing and localization are mediated by different domains of Xist RNA. *Nat Genet* **30**, 167-174, doi:10.1038/ng820 (2002).

63 Luikenhuis, S., Wutz, A. & Jaenisch, R. Antisense transcription through the Xist locus mediates Tsix function in embryonic stem cells. *Mol Cell Biol* **21**, 8512-8520, doi:10.1128/MCB.21.24.8512-8520.2001 (2001).

64 Percharde, M. *et al.* A LINE1-Nucleolin Partnership Regulates Early Development and ESC Identity. *Cell* **174**, 391-405.e319, doi:10.1016/j.cell.2018.05.043 (2018).

65 Maksakova, I. A. *et al.* Distinct roles of KAP1, HP1 and G9a/GLP in silencing of the two-cell-specific retrotransposon MERVL in mouse ES cells. *Epigenetics Chromatin* **6**, 15, doi:10.1186/1756-8935-6-15 (2013).

66 Ding, D. *et al.* The CUE1 domain of the SNF2-like chromatin remodeler SMARCAD1 mediates its association with KRAB-associated protein 1 (KAP1) and KAP1 target genes. *J Biol Chem* **293**, 2711-2724, doi:10.1074/jbc.RA117.000959 (2018).

67 Chao, S. H. & Price, D. H. Flavopiridol inactivates P-TEFb and blocks most RNA polymerase II transcription in vivo. *J Biol Chem* **276**, 31793-31799, doi:10.1074/jbc.M102306200 (2001).

68 Vigneau, S., Augui, S., Navarro, P., Avner, P. & Clerc, P. An essential role for the DXPas34 tandem repeat and Tsix transcription in the counting process of X chromosome inactivation. *Proc Natl Acad Sci U S A* **103**, 7390-7395, doi:10.1073/pnas.0602381103 (2006).

69 Ogawa, Y. & Lee, J. T. Xite, X-inactivation intergenic transcription elements that regulate the probability of choice. *Mol Cell* **11**, 731-743, doi:10.1016/s1097-2765(03)00063-7 (2003).

70 Nesterova, T. B. *et al.* Skewing X chromosome choice by modulating sense transcription across the Xist locus. *Genes Dev* **17**, 2177-2190, doi:10.1101/gad.271203 (2003).

71 Newall, A. E. *et al.* Primary non-random X inactivation associated with disruption of Xist promoter regulation. *Hum Mol Genet* **10**, 581-589, doi:10.1093/hmg/10.6.581 (2001).

72 Vallot, C. *et al.* XACT, a long noncoding transcript coating the active X chromosome in human pluripotent cells. *Nat Genet* **45**, 239-241, doi:10.1038/ng.2530 (2013).

73 Vallot, C. *et al.* XACT Noncoding RNA Competes with XIST in the Control of X Chromosome Activity during Human Early Development. *Cell Stem Cell* **20**, 102-111, doi:10.1016/j.stem.2016.10.014 (2017).

74 Conrad, T. *et al.* Serial interactome capture of the human cell nucleus. *Nat Commun* **7**, 11212, doi:10.1038/ncomms11212 (2016).

75 Chang, C. W. *et al.* Phosphorylation at Ser473 regulates heterochromatin protein 1 binding and corepressor function of TIF1beta/KAP1. *BMC Mol Biol* **9**, 61, doi:10.1186/1471-2199-9-61 (2008).

76 Bunch, H. *et al.* TRIM28 regulates RNA polymerase II promoter-proximal pausing and pause release. *Nat Struct Mol Biol* **21**, 876-883, doi:10.1038/nsmb.2878 (2014).

77 McNamara, R. P. *et al.* KAP1 Recruitment of the 7SK snRNP Complex to Promoters Enables Transcription Elongation by RNA Polymerase II. *Mol Cell* **61**, 39-53, doi:10.1016/j.molcel.2015.11.004 (2016).

78 Bunch, H. *et al.* RNA polymerase II promoter-proximal pausing in mammalian long non-coding genes. *Genomics* **108**, 64-77, doi:10.1016/j.ygeno.2016.07.003 (2016).

79 Tan-Wong, S. M., French, J. D., Proudfoot, N. J. & Brown, M. A. Dynamic interactions between the promoter and terminator regions of the mammalian BRCA1 gene. *Proceedings of the National Academy of Sciences* **105**, 5160-5165, doi:10.1073/pnas.0801048105 (2008).

Methods

Animal care and use

All mice used in the study were housed and bred in the Animal House located at the EMBL Rome (Epigenetics & Neurobiology Unit). All mice were housed in ventilated cages on a standard dark/light cycle. All procedures involving mice adhered to the guidelines in accordance with European Legislation that exists for the protection of animals used for experimental and other scientific purposes (European convention ETS123/Council of Europe, European directive 86/609/EEC and the more recently published Directive 2010/63/EU and its Italian implementation directive 2014/26) as well as the current Guidelines of International Organizations such as the Association for the Assessment and Accreditation of Laboratory Animal Care International - AAALAC and the Federation of European Laboratory Animal Science Association – FELASA.

Mouse cell Lines and derivation of embryonic stem cells

The *Rif1* knockout mouse line was obtained by targeting the *Rif1* locus in Bruce 4 embryonic stem cells. The targeting construct inserts a three-frames STOP cassette and a Neomycin resistance gene, followed by a lox P site into exon 8. Exon 9 is deleted. The targeted cells were screened by PCR and the positive clones verified by Southern blot, following BsrGI and EcoRV digest of the genomic DNA. Two independent clones were injected into blastocysts. Chimeric mice were bred and progeny PCR-genotyped to verify germline transmission. Mice are genotyped using a three-primer PCR Rif1KO comm: 5'-caataccagcctcagctacattc-3'; Rif1 KO wt: 5'-tgtggagtccatgtcttttgc-3'; Rif1 KO2 5'-atagcctgaagaacgagatcagc-3'. Rif1 wild type allele produces a 154 bp band, Rif1 knock-out a 322bp band. $Rif1^{+/-}$ XY^{-sry} Sry^{Tg} mice were obtained by crossing the XY^{-sry} Tg^{Sry} mice[1] to $Rif1^{+/-}$, followed by inter-crosses of the progeny. $Rif1^{F/F}$ $Rosa26^{CreERT/CreERT}$ ($Rs26^{CreERT}$ -*Mus musculus C57BL/6J-129/SvJ*)[2] were crossed with *Mus musculus castaneus* mice and the F1 were inter-crossed for derivation of mESCs of the desired genotypes ($Rif1^{F/F}$ $Rs26^{+/CreERT}$ and $Rif1^{+/+}$ $Rs26^{+/CreERT}$). Derivation of ES cells was carried out according to the protocol as described previously[3-5]. Briefly, Blastocyst outgrowth was cultured on passage 1 Mitomycin C (#M4287, Sigma-Aldrich) -treated primary mouse embryonic fibrobalsts

(pMEFs=feeders) plated at a density of about 350,000 cells/cm^2. First passage disaggregation was performed by mechanical disruption and 0.05% trypsin and the cells re-plated onto feeder coated plates. Once large colonies had formed, they were passaged as ESC lines and expanded in ES medium, Knockout-DMEM (Gibco 10829018), 12.5% heat-inactivated fetal bovine serum (Pan-Biotech), 1% Penicillin/Streptomycin (Gibco 15070063), 1% L-Glutamine (Gibco 25030024), 1% non-essential amino acids (Gibco 11140035), 0.1 mM 2-Mercaptoethanol (Gibco 31350010) and supplemented with 20 ng/ml leukemia inhibitory factor (LIF, EMBL Protein Expression and Purification core facility) and 1 µM MEK inhibitor PD0325901 and 3 µM GSK3 inhibitor CHIR99021 (The University of Dundee, Division of Signal Transduction Therapy)-2i. When cells were stably growing, gelatin adaptation was performed by plating the mESCs on a gelatinised plate (0.1% bovine gelatin in PBS, #G9391 Sigma-Aldrich) with decreasing numbers of feeders. Cells were cultured at 37 °C in 7.5% CO_2. To generate a homogeneous population of cells carrying two X chromosomes, female cell lines with the desired genotype (ESC 34= *Rif1*$^{+/+}$ *Rs26*$^{+/+}$; ESC 15 and ESC 16= *Rif1*$^{F/F}$ *Rs26*$^{+/CreERT2}$, ESC 5= *Rif1*$^{+/+}$ *Rs26*$^{+/CreERT2}$) were sub-cloned by plating cells at very low density on gelatinised tissue culture plates. After 3-5 days, single colonies were picked, expanded and characterized. For knock down studies, the mESC line 34 was used. The Fa2L mESC line[6] used in this study is a subclone (S4) of the Fa2L line (kind gift from P. Avner), adapted to culture in 2i-supplemented medium. The Fa2L line is a female *129/castaneus* hybrid mESC line that carries the insertion of a premature termination site in the *Tsix* gene. As a consequence of this mutation, when these cells are differentiated, the chromosome carrying the mutation (the *129* allele) is almost always selected to become the inactive X chromosome. The Fa2L S4 cell line was maintained on gelatinised plates as described above.

Method details

mESC differentiation

Wild type ESCs were plated onto non-coated petri dishes at a concentration of 1x10^6 cells/ 10 cm^2, in a volume of 10 ml medium lacking 2i and LIF. At day 4 of differentiation the aggregated embryoid bodies (EBs) were gently transferred to gelatinised tissue culture dishes. Medium was gently changed every 48 hours with minimal disruption of

the EBs. EBs were grown for up to 4 or 7 days in total. In experiments where cell differentiation was combined with Rif1 deletion, the differentiation was preceded by 48 hours of 4-hydroxytamoxifen (OHT, #H7904, Sigma-Aldrich) treatment, at a concentration of 200 nM in ES medium containing LIF and 2i. Differentiation was then started with $2x10^6$ cells/ $10cm^2$ dish for *Rif1*$^{+/+}$ and $2.5x10^6$ cells/ $10cm^2$ for *Rif1*$^{F/F}$ cells in medium lacking 2i and LIF but containing 200 nM OHT. At 1 day of differentiation, medium was replaced with medium without OHT. At day 4 of differentiation, the EBs were transferred to gelatinised tissue culture dishes as above.

Whole-mount embryo staining

Embryos were isolated from *Rif1*$^{+/-}$ inter-crossed timed matings at the appropriate day of gestation, by either flushing in M2 medium (Sigma-Aldrich M7167) or by dissection of the uterus and zona pellucida. By mouth-pipetting, the isolated embryos were transferred into fixative (4% PFA in PBS) for 15 minutes (min.) at RT, into wash buffer (3 mg/ml PVP in PBS) and finally into permeabilization buffer (0.25% Triton X-100, #T9284, Sigma-Aldrich in PBS/PVP) for 30 min. All the procedures were performed in siliconized watch glasses. Blocking was performed for 15 min. in 2% donkey serum, 0.1% BSA, 0.01% Tween-20, in PBS (blocking solution). The primary antibodies were diluted as indicated in Supplementary Table 2 in blocking solution and embryos were incubated in primary antibody for 2 days at 4°C. After 3 rinses of 15 min. each in blocking solution, embryos were transferred into secondary antibodies diluted in blocking solution (Molecular Probes Alexa, 1:500) and incubated for 1 hour. After 3 rinses of 15 min. each in blocking solution, the embryos were taken through a series of 25, 50, 75, 100% Vectashield (with or without DAPI). The embryos were mounted in a small drop of Vectashield on a slide surrounded by drops of vaseline. A 13x13mm coverslip was gently lowered on to the vaseline drops and pressed lightly to immobilise the embryos. The coverslips were then sealed with nail varnish. After imaging, the coverslips were gently removed and the embryos recovered by mouth pipetting to be transferred into genotyping buffer (100 mM Tris HCl pH 8, 0.5% igepal (#I3021, Sigma-Aldrich), 0.5% Tween-20, 0.2 mg/mL proteinase K; #P6656, Sigma-Aldrich) and digested at 55 °C at least 3-4 hours. 1 μL of lysate was used for the first of two rounds of nested PCRs to determine the *Rif1* genotype. The sex of the embryos was assigned by H3K27me3 staining of the extra-embryonic tissues.

shRNA Knockdown Experiment

To generate shRNA containing plasmids, double-stranded shRNAs were inserted in between the EcoRI and AgeI sites of pLKO.1 (#8453 and #24150, Addgene), third generation lentivirus vectors carrying resistance marker for puromycin or hygromycin selection respectively. For shRNA sequences see Supplementary Table 1. Correct integration was verified by sequencing.

To generate viruses carrying shRNA constructs, 7.4 x 10^6 HEK239T cells were seeded onto 15cm^2 tissue culture plates and transfected the following day with lentiviral packaging plasmids: 2.6 µg of pMD-HIV1- Gag/Pol, 2.6 µg pRSV-Rev and 5.2 µg of pMD2.G-VSGV, together with 52 µg of pLKO plasmid carrying the desired shRNA sequence, using Ca^{2+}-phosphate transfection method[7]. Medium was changed approximately 16 hours after transfection. The same day of transfection of the packaging cells, 6.5 x10^6 mESC were seeded for infection onto 15cm^2 gelatinised tissue culture plates (for the Fa2L S4 cells: 5.2 x10^6 cells were seeded per 15cm^2 plate). On two subsequent days, starting the day after medium change, viral-containing medium was collected, filtered through a 0.45 µm PES filter, supplemented with Lif and 2i (as described above) and Hexadimethrine bromide (Polybrene, #H9268, Sigma-Aldrich) to a final concentration of 6 µg/ml, and used immediately to transduce the mESCs (days -4 and -3, Fig. 4A). 24 hours following the second transduction (day -2, Fig. 4A) cells were trypsinised and re-plated in medium containing 1µg/ml Puromycin Dihydrochloride (#P8833, Sigma-Aldrich), for selection of cells with stable integration.

For KAP1 knock down in combination with differentiation: the EB differentiation protocol was started at day 2 of puromycin selection (day 0, Fig. 4A). Puromycin was further kept in the medium during the first 24 hours of EB differentiation (day 1, Fig. 4A). Cells were differentiated up to 4 days. For KAP1 knock down and ChIP analysis: puromycin resistant mESCs were collected at day 3 of selection.

For RIF1 knock down in combination with differentiation (Fa2L cells): Fa2L S4 cells were subjected to a second round of infection now using pLKO vectors carrying hygromycin resistance markers. In this second round, mESCs were transduced at day 1 of puromycin selection and day 2 of puromycin selection (=Day 0 EB differentiation). The following day, at day 1 of EB, puromycin was replaced with 180 U/ml of

Hygromycin B *Streptomyces sp* (#400051, Calbiochem), which was kept in the medium for the rest of the experiment. Western blotting was performed to verify the knock down throughout the experiment.

Flavopiridol treatment

Flavopiridol hydrochloride hydrate (#F3055, Sigma-Aldrich) was used to inhibit transcription at a concentration of 500 nM for 4 hours.

KAP1 and RIF1 ChIP

Chromatin immunoprecipitation was performed according to[8]. Briefly, for RIF1 and KAP1 ChIP, collected cells were first crosslinked using 2mM disuccinimidyl glutarate (DSG, # BC366 Synchem UG & Co. KG) in PBS for 45 min. at RT while rotating, washed twice in PBS, followed by 10 min. of additional crosslinking in 1% formaldehyde (#252549, Sigma-Aldrich) in cross-linking buffer (50 mM HEPES pH 7.8, 150 mM NaCl, 1 mM EDTA and 500uM EGTA) at RT. Crosslinking was followed by 5 min. quenching in 0.125 M glycine at RT, washed twice in cold PBS and resuspended in lysis buffer (1% SDS, 10 mM EDTA, 50 mM Tris-HCl pH 8.1, supplemented with protease inhibitor cocktail, #11873580 001, Roche). Chromatin fragmentation was performed using Soniprep 150 to produce a distribution of fragments enriched between 300 and 400 bp. The lysate was precleared by centrifugation at low speed 200 rpm for 20 min at 4 °C. Chromatin was quantified using Qubit dsDNA High Sensitivity assay kit (#Q32854, Life Technologies). Immunoprecipitation was performed by incubating 100 µg of chromatin diluted in 10 volumes of Dilution buffer (1% Triton X-100, 2 mM EDTA, 167 mM NaCl, 20 mM Tris-HCl pH 8.1, including Protease Inhibitor) overnight rotating at 4 °C together with either α-KAP1 or α-RIF1 antibodies (see Supplementary Table 2) or IgG only control (#sc-2026, Santa Cruz), 10% of chromatin was isolated as input control. The following day, 50 µl of Dynabeads protein G slurry (#10004D, Thermo Fisher) per ChIP sample was added and incubated rotating for another 2 hours at 4 °C. The beads were magnet-separated and washed twice with Low salt buffer (0.1% SDS, 1% Triton X-100, 2 mM EDTA, 150 mM NaCl, 20 mM Tris-HCl pH8.1), one time each with High salt buffer (0.1% SDS, 1% Triton X-100, 2 mM EDTA, 500 mM NaCl, 20 mM Tris-HCl pH8.1), LiCl buffer (0.25M LiCl, 0.5% NP-40, 0.5% sodium deoxycholate, 1mM EDTA,10 mM Tris-HCl pH 8.1) and

finally TE. Each wash was performed for 5 min. on a rotating wheel at 4 °C and all buffers were supplemented with protease inhibitor cocktail (#11873580 001, Roche). Prior to elution, samples were rinsed once in TE without protease inhibitor. ChIP-DNA was eluted from the beads by rotating at RT for 1 hour in Elution buffer (1% SDS, 100 mM $NaHCO_3$). Beads were separated and the supernatants as well as input samples were subjected to RNAse A (#R5250, Sigma-Aldrich) treatment (1.5µl/sample) for 1 hour at 37 °C followed by decrosslinking using Proteinase K (#P6556, Sigma-Aldrich) treatment (45µg/sample) overnight at 60 °C. The following day, ChIP-DNA and input samples were purified using ChIP DNA Clean and Concentrator kit (#D5205, Zymo Research) and retrieved DNA as well as input DNA was quantified using Qubit dsDNA High Sensitivity assay kit (#Q32854, Life Technologies). The concentration of ChIP-DNA and input samples were adjusted to maintain a similar ratio of ChIP-DNA:INPUT between different ChIP experiments. qPCRs were performed using the SYBR Green reaction mix (#04887352001, Roche) on a LightCycler 96 Instrument (Roche), following standard protocols. Enrichments over input control were calculated for each respective primer set. Primer sequences are presented in Supplementary Table 3.

YY1 ChIP

Cells were collected and crosslinked in 1% formaldehyde in cross-linking buffer (50 mM HEPES pH 7.8, 150 mM NaCl, 1 mM EDTA and 500uM EGTA) for 30 min. at 37 °C. Crosslinking was followed by 5 min. quenching in 0.125 M glycine at RT, washed twice in cold PBS and resuspended in lysis buffer (1% SDS, 10 mM EDTA, 50 mM Tris-HCl pH 8.1, supplemented with protease inhibitor cocktail, #11873580 001, Roche). Chromatin fragmentation was performed using a Bioruptor sonication device (Diagenode) to produce a distribution of fragments enriched between 200 and 300 bp. Immunoprecipitation was performed as described for KAP1 and RIF1 ChIP using α-YY1 antibody (see Supplementary Table 2) and IgG only control. ChiP-qPCR primers are presented in Supplementary Table 3.

Protein extraction, SDS-PAGE and western blotting

Cells were collected, washed once with cold PBS and resuspended in 2x Laemmli buffer at 10,000 cells/ ul. Samples were homogenised using D Micro-Fine 1ml Insulin Syringe with 29G x 12.7mm Needle (#324891, Becton Dickinson) and boiled for 7-

10min. Proteins were resolved by 5% (RIF1, KAP1 and SMC1) and 10% (RNF12 and LMNB1) SDS-PAGE, transferred to 0.45 μm nitrocellulose membrane (#10600002, Amersham), overnight at 4 °C in transfer buffer (390 mM Glycine, 48 mM Tris base, 0.1% SDS and 20% Methanol) or 3 hours (1x Tris-Glycine buffer supplemented with 20% methanol) using standard procedures. Following transfer, membranes were blocked with 5 % (w/v) skim milk powder (#84615.0500, VWR) in 0.05% (v/v) Tween-TBS (TBS-T) for a minimum of 30 min. at RT. Membranes were incubated either overnight at 4 °C or 3 hours at RT with antibodies (see Supplementary Table 2) diluted in blocking buffer or 2.5% milk/ TBS-T. Secondary antibodies were diluted 1:15,000 in 2.5% milk/ TBS-T and incubated for approximately 45 min. Secondary antibodies were as follow: Donkey Anti-Rabbit IgG Antibody IRDye:800CW Conjugated (#926-32213, LI-COR Biosciences), Donkey Anti-Rabbit IgG Antibody IRDye:680RD Conjugated (#925-68073, LI-COR Biosciences). Goat Anti-Mouse IgG Antibody IRDye:800CW Conjugated (#925-32210, LI-COR Biosciences). Blots were imaged with Odyssey® CLx Imager (LI-COR Biosciences) and the intensity of each band was quantified using the Odyssey imaging software.

Nuclear-Cytoplasmic Fractionation

Cell fractionation and solubilisation of chromatin-bound proteins by salt extraction was performed according to[9]. Briefly, mESCs were harvested, washed 2x in PBS and resuspended in cold Buffer A (10mM HEPES pH 7.9, 10mM KCl, 1.5mM $MgCl_2$, 0.34M sucrose, 10% glycerol, 1mM DTT with freshly added Protease (#11873580 001, Roche) and Phosphatase Inhibitors) at 4x 10^7 cells/μl making sure no cell clumps remain. Triton X-100 to a final concentration of 0.1% was added slowly, swirling the pipet tip from bottom to top. Samples were incubated 5 min. on ice followed by a centrifugation for 4 min. at 1300 g, 4 °C. The supernatant, containing the cytosolic fraction (S1) was collected and spun in an ultracentrifuge at 20000g for 15 min. and the S1-pellet was resuspended in 2x Laemmli buffer. The remaining nuclear pellet (P1) was gently washed in 500μL Buffer A and centrifuged 4 min. at 1300 g, 4 °C. The washed P1-pellet was resuspended in a volume of Buffer B (3mM EDTA, 0.2mM EGTA, 1mM DTT with freshly added Protease and Phosphatase Inhibitors) equal to the initial Buffer A and incubated on ice for 30 min. Incubation was followed by a centrifugation for 4 min. at 1700 g, 4 °C. The supernatant, containing the soluble

nucleoplasmic fraction (P2) was collected, spun down and resuspended in 2x Laemmli buffer. The pellet, containing the nuclear pellet+chromatin fraction (P3) was resuspended in a volume of 2x Laemmli buffer equal to the initial buffer A volume. All samples were syringed through a D Micro-Fine 1ml Insulin Syringe with 29G x 12.7mm needle and boiled for 7-10 min.

RNA extraction, reverse transcription and RT-qPCR

Frozen cell pellets were lysed and homogenised using QIAshredder column (#79656, QIAGEN) followed by RNA extraction using the RNeasy kit (#74106, QIAGEN) according to the manufacturer's instructions. On column-DNAse treatment was performed at 25 °C-30 °C for 20 min. using RQ1 RNase-Free DNase (#M6101, Promega). After elution, a second round of DNAse treatment was performed using 8U of DNase/sample, incubated at 37 °C for 20 min. The reaction was terminated by adding 1µl of RQ1 DNase Stop Solution and incubate at 65 °C for 10 min. RNA was quantified using Nanodrop, and cDNA synthesis was performed using RevertAid H Minus First Strand cDNA kit (#K1632, Thermo Scientific) using random hexamer priming. qPCRs were performed using the SYBR Green reaction mix (#04887352001, Roche) on a LightCycler 96 Instrument, following standard protocols. Gene expression data was normalised against a geometric mean generated by RT-qPCR of either: *Gapdh*, *Ubiquitin* and *β-Actin* or *Rplp0*, *Ubiquitin* and *Sdha*. For flavopiridol treated cells, gene expression levels were normalised against *18S* ribosomal RNA. Primers for RT-qPCR are listed in Supplementary Table 4. Absolute expression levels were calculated using the Ct ($2^{-\Delta Ct}$) method and relative levels using Ct ($2^{-\Delta\Delta Ct}$) [10].

Immunofluorescence

mESCs were plated on gelatinised coverslips overnight. For differentiated cells, at the day of harvest, the embryoid bodies were gently disrupted into single cells using 0.05% Trypsin-EDTA and mechanical dissociation, then cytospun onto polysine coated slides (#J2800AMNZ, Thermo Scientific) at 1000 rpm for 5 min. Cells were fixed in 4% paraformaldehyde in PBS for 10 min. at RT and stored at 4 °C in PBS. For staining, coverslips were permeabilized in 0.5% Triton X-100/ PBS at RT for 10 min., washed x2 with PBS/ 0.2% Tween-20 and blocked for 30 min. in 1% BSA/ PBS/ 0.02% Tween-20. Primary antibody was diluted in 0.5% BSA/ PBS/ 0.02% Tween-20 and coverslips

were incubated on for 3 hours at RT. After x3 washes in PBS/ 0.02% Tween-20, coverslips were incubated with secondary antibody, Alexa-488 Donkey anti-Rabbit antibody (#A21206, Thermo Fisher) diluted 1:800 in 0.5% BSA/ PBS/ 0.2% Tween-20, for 45 min. at RT in the dark. Following x3 washes in PBS/ 0.02% Tween-20 and x1 wash in PBS, coverslips were mounted with Vectashield including DAPI (#H-1200, Vector Laboratories). Images were acquired using a Zeiss Axio Imager. Cell count minimum of 100 cells /slide.

Methods references

1 De Vries, G. J. *et al.* A model system for study of sex chromosome effects on sexually dimorphic neural and behavioral traits. *J Neurosci* **22**, 9005-9014 (2002).

2 Buonomo, S. B., Wu, Y., Ferguson, D. & de Lange, T. Mammalian Rif1 contributes to replication stress survival and homology-directed repair. *J Cell Biol* **187**, 385-398, doi:10.1083/jcb.200902039 (2009).

3 Foti, R. *et al.* Nuclear Architecture Organized by Rif1 Underpins the Replication-Timing Program. *Mol Cell* **61**, 260-273, doi:10.1016/j.molcel.2015.12.001 (2016).

4 Bryja, V., Bonilla, S. & Arenas, E. Derivation of mouse embryonic stem cells. *Nat Protoc* **1**, 2082-2087, doi:10.1038/nprot.2006.355 (2006).

5 Bryja, V. *et al.* An efficient method for the derivation of mouse embryonic stem cells. *Stem Cells* **24**, 844-849, doi:10.1634/stemcells.2005-0444 (2006).

6 Luikenhuis, S., Wutz, A. & Jaenisch, R. Antisense transcription through the Xist locus mediates Tsix function in embryonic stem cells. *Mol Cell Biol* **21**, 8512-8520, doi:10.1128/MCB.21.24.8512-8520.2001 (2001).

7 Graham, F. L. & van der Eb, A. J. A new technique for the assay of infectivity of human adenovirus 5 DNA. *Virology* **52**, 456-467, doi:10.1016/0042-6822(73)90341-3 (1973).

8 Bulut-Karslioglu, A. *et al.* A transcription factor-based mechanism for mouse heterochromatin formation. *Nat Struct Mol Biol* **19**, 1023-1030, doi:10.1038/nsmb.2382 (2012).

9 Mendez, J. & Stillman, B. Chromatin association of human origin recognition complex, cdc6, and minichromosome maintenance proteins during the cell cycle: assembly of prereplication complexes in late mitosis. *Mol Cell Biol* **20**, 8602-8612, doi:10.1128/mcb.20.22.8602-8612.2000 (2000).

10 Livak, K. J. & Schmittgen, T. D. Analysis of relative gene expression data using real-time quantitative PCR and the 2(-Delta Delta C(T)) Method. *Methods* **25**, 402-408, doi:10.1006/meth.2001.1262 (2001).

FIGURE 1

A

C57BL/6J: *Rif1*$^{+/-}$ x *Rif1*$^{+/-}$

Rif1	+/+		+/-		-/-	
	F	M	F	M	F	M
observed	61	57	64*	105	0	1
expected	59	59	118	118	59	59

* P value=0.002

B

C57BL/6J-129/Sv: *Rif1*$^{+/-}$ x *Rif1*$^{+/-}$

Rif1	+/+		+/-		-/-	
	F	M	F	M	F	M
observed	46	45	103	118	0	15
expected	45.5	45.5	91	91	45.5	45.5

C

C57BL/6J: *Rif1*$^{+/-}$ x *Rif1*$^{+/-}$

Rif1	+/+	+/-	-/-		
			F	M	Tot
E5.5	9	16	3	1	4
E6.5	14	33	6	4	10
E7.5	7	32	4#	3	7
E10.5	12	23	0	5#	5

#abnormal

D

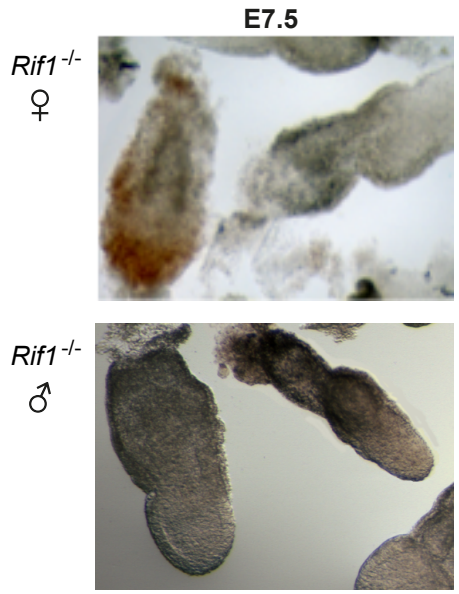

FIGURE 2

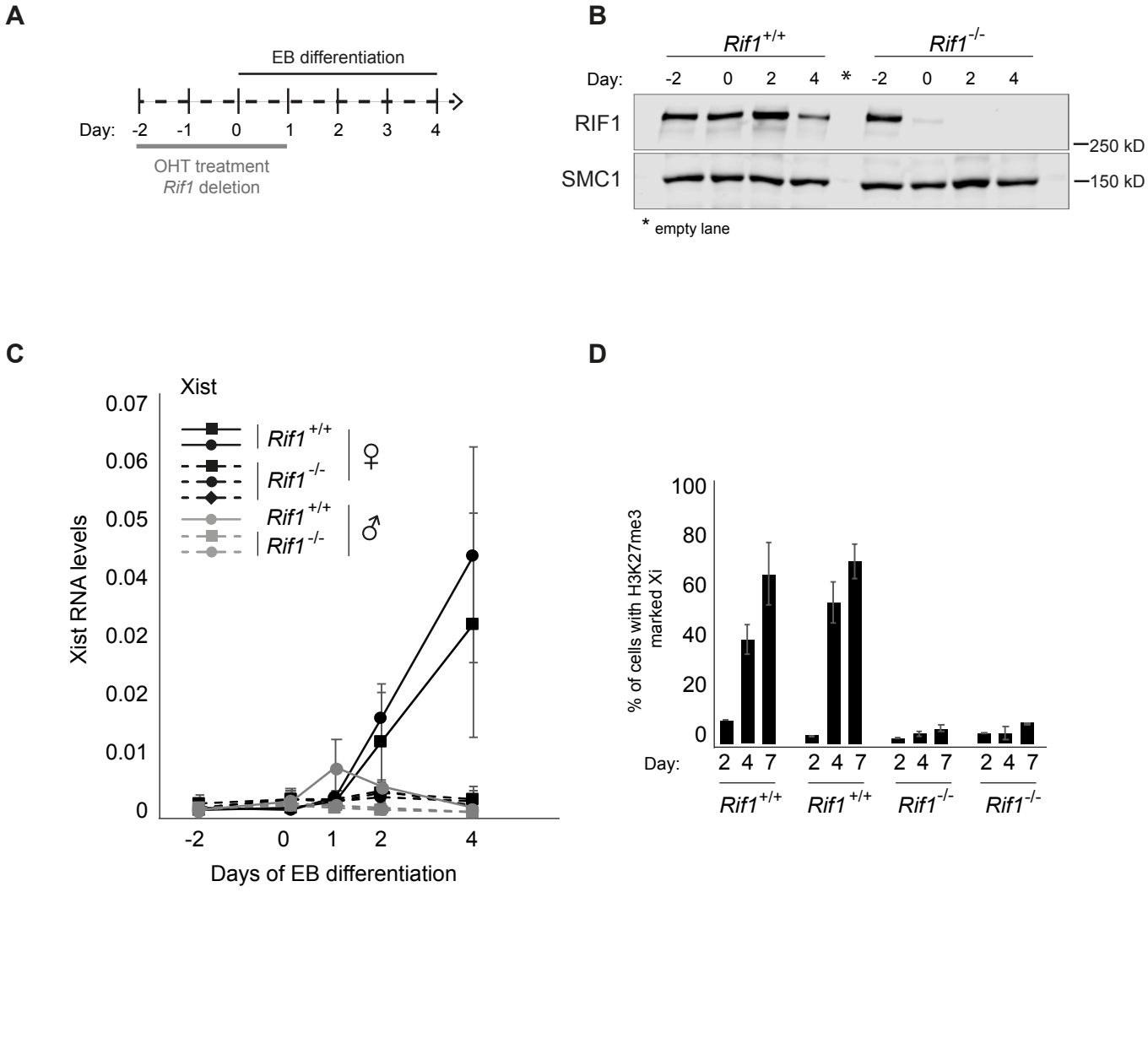

FIGURE 3

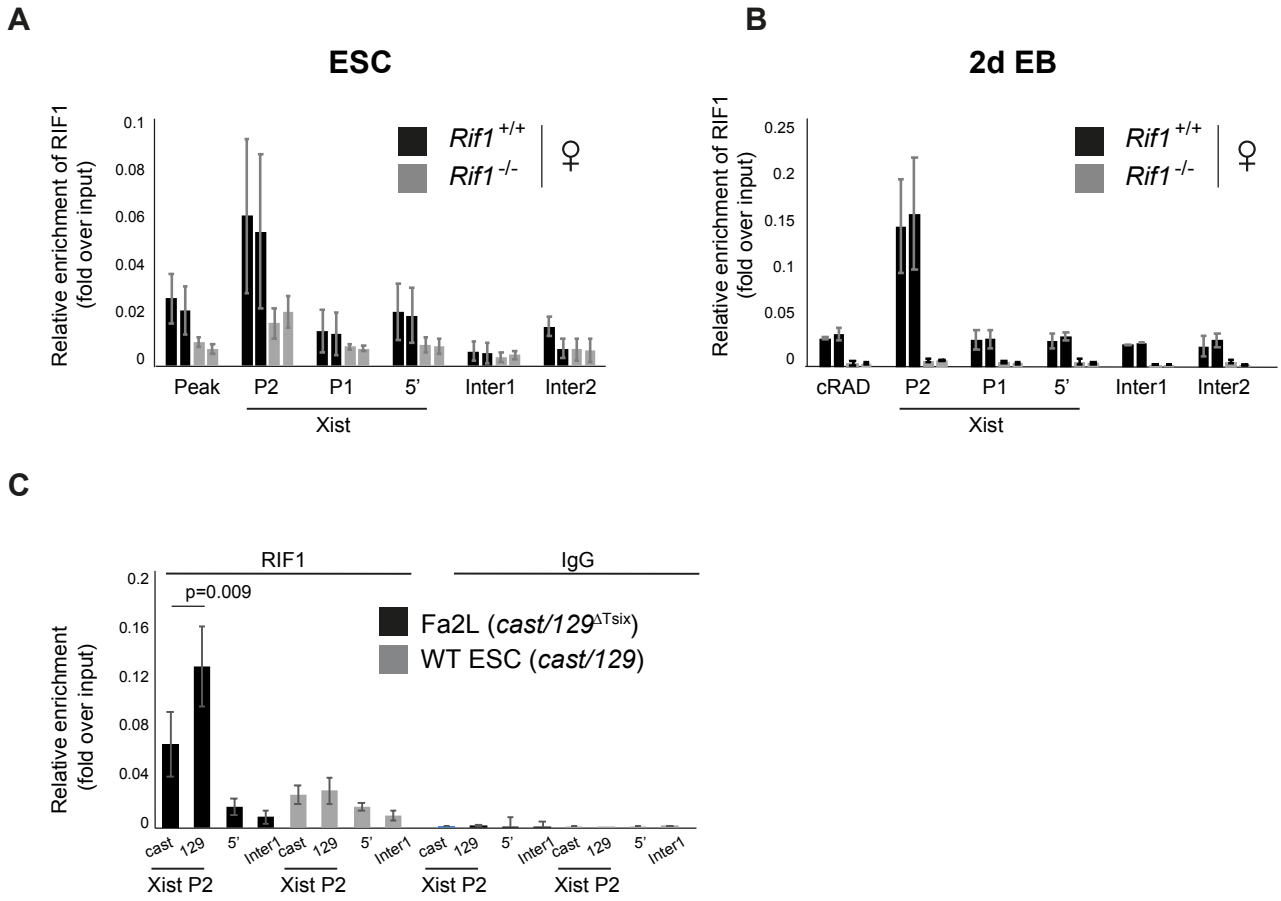

FIGURE 4

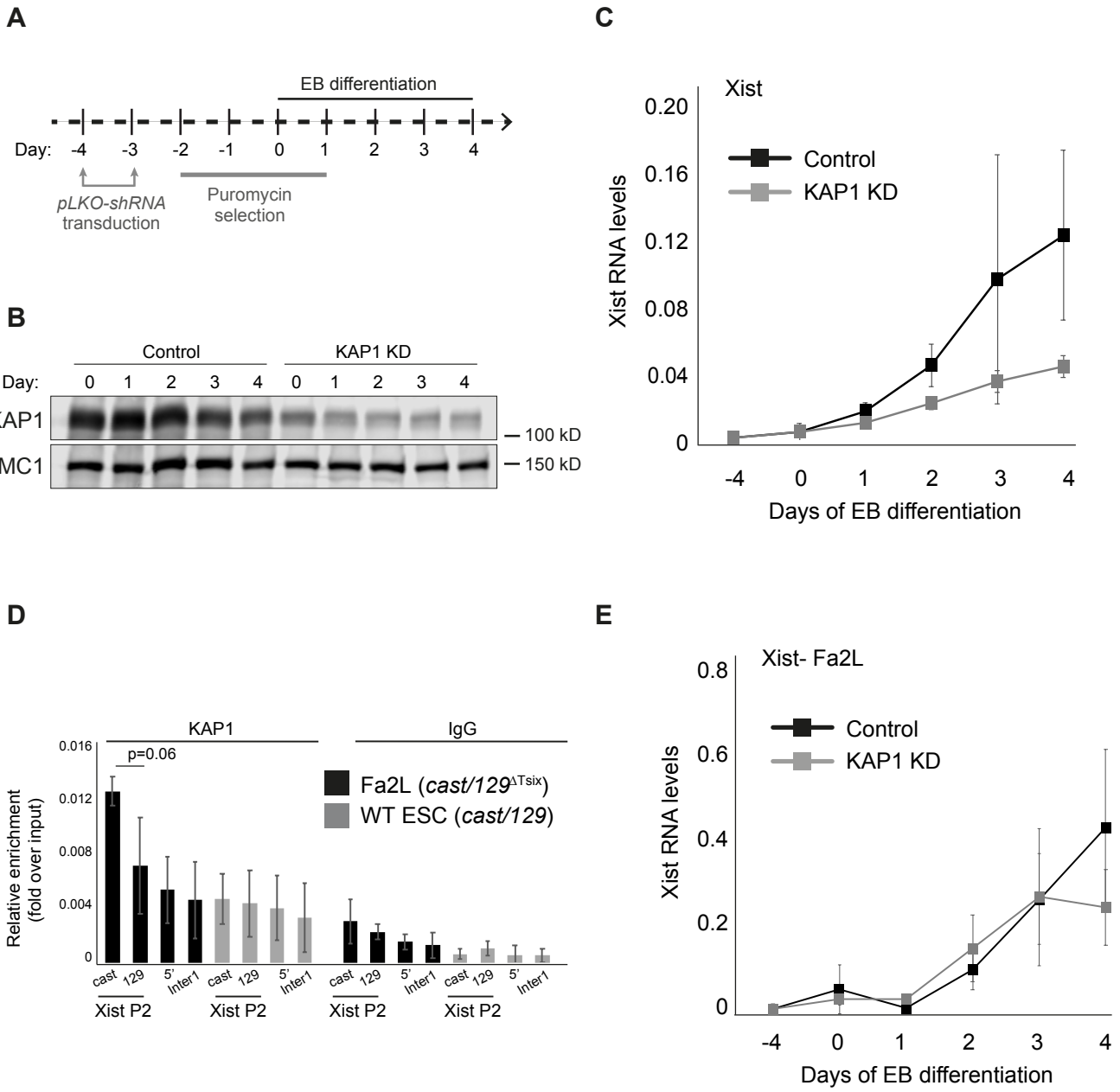

FIGURE 5